Two Types of Potassium Channels in Murine T Lymphocytes

T. E. DECOURSEY, K. G. CHANDY, S. GUPTA, and M. D. CAHALAN

From the Departments of Physiology and Biophysics and of Medicine, University of California, Irvine, California 92717, and the Department of Physiology, Rush-Presbyterian-St. Luke's Medical Center, Chicago, Illinois 60612

ABSTRACT The properties of two types of K^+ channels in murine T lymphocytes are described on the basis of whole-cell and isolated-patch recordings using the gigohm-seal technique. Type *l* (standing for "*lpr* gene locus" or "large") channels were characterized mainly in T cells from mutant MRL/MpJ-*lpr/lpr* mice, in which they are present in large numbers. Type *n* ("normal") K^+ channels are abundant and therefore most readily studied in concanavalin A–activated T cells from four strains of mice, MRL-+/+, CBA/J, C57BL/6J, and BALB/c. Type *l* channels, compared with type *n*, are activated at potentials ~30 mV more positive, and close much more rapidly upon repolarization. Type *l* channels inactivate more slowly and less completely than type *n* during maintained depolarization, but recover from inactivation more rapidly, so that little inactivation accumulates during repetitive pulses. Type *l* channels have a higher unitary conductance (21 pS) than type *n* (12 pS) and are less sensitive to block by external Co^{++}, but are 100-fold more sensitive to block by external tetraethylammonium (TEA), with half-block of type *l* channels at 50–100 μM TEA compared with 8–16 mM for type *n*. TEA blocks both types of channels by reducing the apparent single channel current amplitude, with a dose-response relation similar to that for blocking macroscopic currents. Murine type *n* K^+ channels resemble K^+ channels in human T cells.

INTRODUCTION

Voltage-gated K^+ channels have been found in patch-clamp studies in a variety of cells of the immune system. K^+ channels are present in most T lymphocytes and T lymphocyte–related cell lines and in natural killer cells (DeCoursey et al., 1984*a*, 1985*c*; Matteson and Deutsch, 1984; Fukushima et al., 1984; Cahalan et al., 1985; Lee et al., 1986; Schlichter et al., 1986). In macrophages and in a macrophage-derived cell line, K^+ channels are absent in freshly plated cells, but appear in large numbers after the cells adhere to the substrate (Ypey and Clapham, 1984; Gallin and Sheehy, 1985). The macroscopic and microscopic properties of K^+ channels described in all of these cells are similar: the K^+

Address reprint requests to Dr. Thomas E. DeCoursey, Dept. of Physiology, Rush University, 1750 W. Harrison, Chicago, IL 60612.

J. GEN. PHYSIOL. © The Rockefeller University Press · 0022-1295/87/03/0379/26$1.00

Volume 89 March 1987 379–404

conductance is activated with a sigmoid time course upon depolarization to potentials positive to about −40 mV, inactivated slowly during maintained depolarization, and blocked by externally applied tetraethylammonium (TEA) or 4-aminopyridine (4-AP). The channel is voltage-gated and is not activated by internal free Ca^{++} levels within the physiological range. Unitary K^+ currents exhibit "flicker" and correspond to a conductance of 10–20 pS at a physiological K^+ concentration.

Several types of evidence suggest that K^+ channels play a role during activation and proliferation of T lymphocytes (DeCoursey et al., 1984*a*; Chandy et al., 1984; Cahalan et al., 1985). With this in mind, we have studied a strain of mice that homozygously express the autosomal recessive mutant *lpr* gene locus, MRL/MpJ-*lpr/lpr* (MRL-*l*) (Chandy et al., 1986). These mice develop severe lymphoproliferation of functionally and phenotypically abnormal T lymphocytes (Murphy, 1981; Altman et al., 1981; Wofsy et al., 1981). We studied the congenic strain MRL/MpJ-+/+ (MRL-*n*) and several other "normal" strains that do not develop lymphoproliferation as a source of control cells. In the course of this study, we discovered that there are two distinct kinds of K^+ channels in murine T cells. One, which we call type *n* (for "normal"), resembles the K^+ channels found in other cells of the immune system. The K^+ conductance of T lymphocytes from MRL-*l* mice reflected a very different type of K^+ channel, called type *l*. Type *l* channels were named for the *lpr* mouse strain in which they were initially found (Chandy et al., 1986), but they are also present in other strains, so a better mnemonic device is "large," because of their larger single channel conductance. In this article, we describe the properties of these two K^+ channels.

Preliminary accounts of this work have been presented (DeCoursey et al., 1985*a*, *b*).

METHODS

Preparation

C57BL/6J and C3H/HeJ mice were purchased from The Jackson Laboratory, Bar Harbor, ME; CBA/J mice were purchased from the Scripps Immunology Research Institute, La Jolla, CA; BALB/c mice were from a colony maintained by the Dept. of Microbiology, University of Califoria at Irvine. T cell preparations from MRL-*l*, MRL-*n*, and some C57BL/6J mice were generously provided by Dr. M. Fischbach (Audie Murphy Veterans Administration Hospital, University of Texas at San Antonio). The MRL-*l* mice studied were 1.5 mo old ("young") or 4–7.5 mo old ("old"); MRL-*n* mice were 1.5–7 mo old; and mice from other strains were 2–4 mo old. Both male and female mice were used. The MRL-*l* and MRL-*n* strains have gone through at least 10 cycles of cross-intercross matings and the residual heterozygosity is <0.1% (Murphy, 1981); on this basis, they are considered to be congenic.

T cells were isolated from single-cell suspensions prepared from lymph nodes or spleens, by passage through a nylon wool column. Splenic T cells were used for all CBA/J, BALB/c, and C3H/HeJ experiments; lymph node T cells were used for all C57BL/6J mouse studies. T cell preparations were >98% viable as determined by trypan blue dye exclusion.

TEA, purchased from Eastman Kodak Co. (Rochester, NY), and 4-AP, from Sigma Chemical Co. (St. Louis, MO), were recrystallized before use. Verapamil, nifedipine, and

diltiazem were generously provided by Dr. R. W. Tsien (Yale University, New Haven, CT); cetiedil was provided by Dr. L. R. Berkowitz (University of North Carolina, Chapel Hill, NC).

Voltage-Clamp Experiments

Details of the gigohm-seal voltage-clamp technique used here are described elsewhere (DeCoursey et al., 1984*a*; Cahalan et al., 1985). Briefly, most cells were studied in the whole-cell configuration, in a mammalian Ringer solution containing (mM): 160 Na^+, 4.5 K^+, 2 Ca^{++}, 1 Mg^{++}, 170.5 Cl^-, and 5 HEPES, titrated to pH 7.4 with NaOH. The pipette solution contained 162 K^+, 1 Ca^{++}, 1 Mg^{++}, 140 F^-, 11 EGTA, and 10 HEPES, titrated to pH 7.2 with NaOH or tetramethylammonium (TMA)-OH; in a few experiments, F^- was replaced by aspartate$^-$. All experiments were performed at room temperature (20–23°C). Electrodes were coated with Sylgard (Dow Corning Corp., Midland, MI) and fire-polished to resistances, measured in the bath, of 3–8 MΩ. Most experiments were carried out using an L/M EPC-7 patch clamp (Medical Systems Corp., Great Neck, NY). Series resistance compensation was usually increased until the current during a voltage step neared oscillation and then was set just below this point (at ~50% compensation). The small amplitude of currents in most experiments minimized errors caused by series resistance. The absolute potential was established as the zero-current potential with the electrode in the bath in Ringer solution. Potentials are given without correction for the junction potential between Ringer and the pipette solution; all stated potentials can be corrected by subtracting 4–5 mV. After achieving the whole-cell configuration, at least 10 min was allowed for equilibration, to allow the voltage dependence of various parameters to stabilize (Marty and Neher, 1983; Fernandez et al., 1984; Cahalan et al., 1985).

Experiments were performed on-line with an LSI-11/23 computer. Current data were digitized and stored in files for off-line analysis. Fitting was carried out either by analog adjustment of parameters or by nonlinear least squares. For the latter, the standard deviation of the parameter in the fit provides a measure of the extent to which each fitted parameter is defined by the data. The significance of differences between mean parameter values was calculated by Student's *t* test.

RESULTS

Voltage-gated K^+ channels were present in almost every T lymphocyte from all strains of mice studied. The outward current during depolarizing voltage pulses is carried by K^+, as indicated by the dependence of the reversal potential upon the external K^+ concentration (data not shown). Two different types of K^+ channels are present in murine T cells. Both the type and number of K^+ channels per cell depend upon the strain of mouse and the state of activation of the cells (DeCoursey et al., 1987). Type *l* channels were primarily characterized in MRL-*l* T cells, whereas type *n* channels were studied mainly in concanavalin A (Con A)–activated "normal" T cells. The properties of both types of channels are shown to be independent of the strain of mouse. In this article, the properties of these two types of K^+ channels are compared.

TEA Sensitivity of K^+ Currents

One of the most striking differences between the two types of K^+ channels is in their sensitivity to block by external TEA. Fig. 1 illustrates the block of K^+ currents in an MRL-*l* cell (*A*) and in an MRL-*n* cell (*B*) exhibiting identical high sensitivity to TEA. The MRL-*n* cell in Fig. 1 *C* illustrates a much lower sensitivity

to TEA. Normalized currents from these experiments are plotted in Fig. 1 *D*, along with dose-response curves corresponding to half-blocking concentrations of 60 μM and 13 mM TEA. In most cells studied, the block of the K^+ conductance, g_K, by TEA reflected predominantly only one or the other of these sensitivities; half-block in a given cell generally occurred either at 50–100 μM or at 8–16

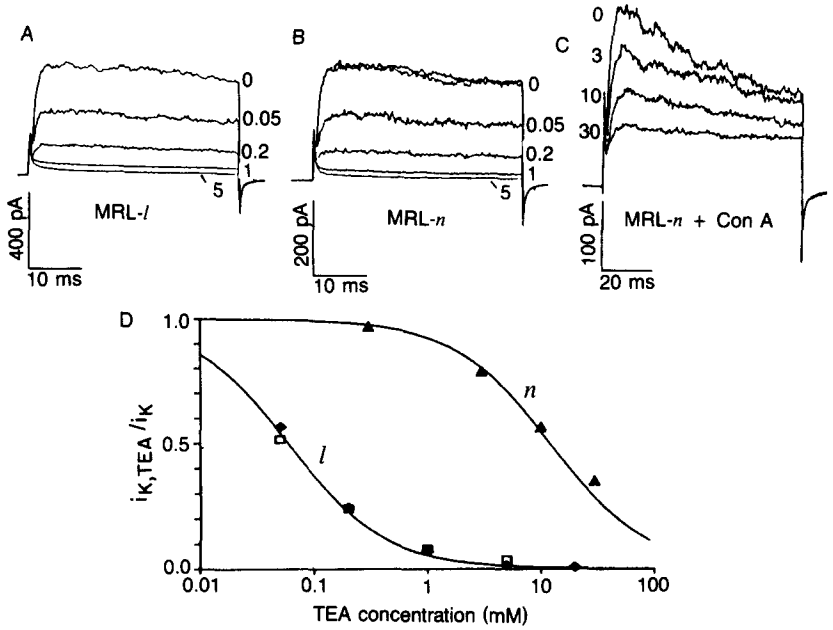

FIGURE 1. (*A–C*) Block of whole-cell K^+ currents by TEA added to the bath in Ringer solution at the indicated concentrations (in millimolar). Brief test pulses to +40 mV were applied every 30 s from a holding potential of −80 mV. (*A*) An MRL-*l* lymph node T cell in the presence of 0, 0.05, 0.2, 1, or 5 mM TEA, exhibiting type *l* high TEA sensitivity. (*B*) An MRL-*n* lymph node T cell exhibiting high TEA sensitivity. Control records taken before and after application of TEA are superimposed. (*C*) An MRL-*n* T cell, incubated with Con A for 54 h, illustrating low (type *n*) sensitivity to TEA. TEA concentrations are 0, 3, 10, and 30 mM, with the control (0 mM TEA) record taken after washout of TEA. (*D*) TEA dose-response relations for block of whole cell K^+ currents shown in *A* (◆), *B* (□), and *C* (▲). Currents in the presence of TEA were normalized with respect to the means of control currents before and after application of TEA, all after subtraction of a linear leak current. The smooth curves show block for one TEA molecule to one K^+ channel stoichiometry, with half-block at 60 μM and 13 mM.

mM TEA. In some cells, the dose-response data could be fitted by assuming that both types of channels were present in the same cell, but in nearly all of these cells, the predominant channel accounted for 80–90% or more of the total g_K, so that the minor component could not be distinguished clearly. Evidence confirming the coexistence of type *n* and type *l* K^+ channels in individual cells is presented below.

The two-order-of-magnitude difference in TEA sensitivity provides a clear pharmacological distinction between the two types of K^+ channels, which was consistently paralleled by several kinetic features of the channels' gating and by differences in single channel conductance. For conciseness, we designate cells whose g_K is comprised mainly of type *l* K^+ channels as type *l* cells, and cells with mainly type *n* K^+ channels as type *n* cells. Briefly, the g_K in cells with high TEA sensitivity (type *l* cells), compared with type *n* cells, always exhibited rapid tail current kinetics, slow and incomplete inactivation, little or no accumulation of inactivation during repetitive pulses, and activation at more positive potentials.

Voltage Dependence of g_K

In cells with a reasonably large g_K, the relationship between peak g_K and voltage (V) was quantified by fitting the data, by nonlinear least squares, with a Boltzmann function:

$$g_K(V) = \frac{g_{K,max}}{1 + \exp[(V - V_n)/k_n]}, \quad (1)$$

and adjusting the maximum available K^+ conductance, $g_{K,max}$, the half-activation potential, V_n, and k_n, which expresses the steepness of the voltage dependence. Most cells were fitted fairly well by Eq. 1, as shown for an MRL-*l* T cell by the dotted curve in Fig. 2*A*. Fig. 2*B* shows g_K-V curves drawn from mean parameter values for similarly fitted data from type *l* MRL-*l* T cells and type *n* Con A–activated MRL-*n* T cells. Type *l* channels are activated at ~30 mV more positive potentials than are type *n*. Table I summarizes the voltage dependence of g_K in resting and activated T cells classified as mainly type *l* or type *n*, from several strains. Macroscopic currents were analyzed in a few resting MRL-*n* cells with a sizable g_K, which were mainly type *l* cells. The parameter values for these type *l* MRL-*n* T cells in Table I are very similar to those in MRL-*l* T cells, which supports the idea that type *l* channels in both strains are the same. Table I also shows that the predominant K^+ channels in Con A–activated T cells from other normal murine strains displayed a voltage dependence very similar to that in Con A–activated MRL-*n* T cells. This result, in addition to the low TEA sensitivity shared by Con A–activated T cells from C57BL/6J, CBA/J, BALB/c, and MRL-*n* mice, suggests that the type *n* channels from different strains are the same.

In some type *l* MRL-*n* or MRL-*l* T cells (e.g., Fig. 2*C*), the peak g_K-V relation displayed a small hump around −40 to −20 mV. Although this hump was usually not very pronounced in MRL-*l* T cells such as the one in Fig. 2*A*, the gradual voltage dependence of g_K around "threshold" potentials in MRL-*l* T cells is in striking contrast to the steep voltage dependence of g_K near threshold in human T lymphocytes (DeCoursey et al., 1984*a*; Cahalan et al., 1985). In cells in which the peak g_K-V relation appeared to be bimodal, the data were fitted to the sum of two Boltzmann terms (shown by the solid curves in Fig. 2, *A* and *C*):

$$g_K(V) = \frac{g_{K,1}}{1 + \exp[(V - V_{n,1})/k_{n,1}]} + \frac{g_{K,2}}{1 + \exp[(V - V_{n,2})/k_{n,2}]}, \quad (2)$$

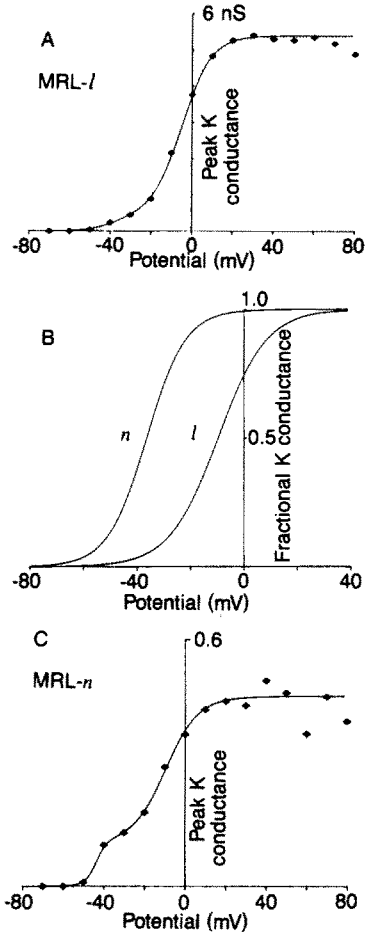

FIGURE 2. Voltage dependence of g_K in type n and type l cells.The chord conductance is plotted since the instantaneous current-voltage relation in both type l and type n murine K^+ channels appears to be roughly linear in the solutions used, as shown previously for human T cell K^+ channels (Cahalan et al., 1985). (*A*) Type l whole-cell peak g_K in an MRL-l lymph node T cell during depolarizing steps from −80 mV to the potentials on the abscissa. The dotted curve shows the best-fitting Boltzmann function (Eq. 1), with $V_n = -7.1 \pm 0.4$ mV (± SD in the fit), $k_n = -8.2 \pm 0.4$ mV, and $g_{K,max} = 5.36 \pm 0.04$ nS. The solid curve shows the sum of two Boltzmann terms (Eq. 2), with $V_{n,1} = -36.8$ mV, $k_{n,1} = -6.9$ mV, $g_{K,1} = 0.4$ nS, $V_{n,2} = -4.1$ mV, $k_{n,2} = -7.3$ mV, and $g_{K,2} = 5.0$ nS. (*B*) Average g_K-V relations plotted from the mean parameter values (given in Table III) of simple Boltzmann fits (Eq. 1) to $g_K(V)$ in MRL-l cells, (*l*) and in MRL-n cells activated with Con A, and judged by independent criteria to be predominantly type n. (*C*) Bimodal whole-cell peak g_K in an MRL-n cell. The curve shows the sum of two Boltzmann terms (Eq. 2) with $V_{n,1} = -43$ mV, $k_{n,1} = -2.6$ mV, $g_{K,1} = 0.11$ nS, $V_{n,2} = -9$ mV, $k_{n,2} = -8.2$ mV, and $g_{K,2} = 0.36$ nS. Recorded 16 min after establishing the whole-cell configuration; the reversal potential was assumed to be −80 mV.

where the parameters for each component are analogous to those in Eq. 1. The mean parameters in MRL-*l* and MRL-*n* cells judged to have bimodal g_K-V curves are included in Table I. In eight MRL-*l* cells, the smaller component averaged 0.09 ± 0.02 (SE) the amplitude of the larger one. The simplest interpretation of these data is that both types of K^+ channels are present: a small number of type *n* channels that activate around −40 mV, and a much larger population of type *l* channels that activate at more positive potentials. The parameter values in Table I for the small and large components of the g_K in cells from MRL cells with bimodal g_K-V curves are in good agreement with the values for type *n* and type *l* channels, respectively, in cells with predominantly only one type of channel. Theoretical K^+ conductance-voltage curves, calculated assuming that various proportions of type *l* and type *n* K^+ channels are present in the same cell,

TABLE I

Voltage Dependence of Type n and Type l K^+ Channels

				Type *n*			Type *l*		
Strain	Con A	Type	*n*	$V_{n,1}$	$k_{n,1}$	$g_{K,1}$	$V_{n,2}$	$k_{n,2}$	$g_{K,2}$
				mV	*−mV*	*nS*	*mV*	*−mV*	*nS*
MRL-*l*	No	*l*	18	—	—	—	−4±2	9.2±0.3	5.1
MRL-*l*	Yes	*l*	4	—	—	—	2±4	9.5±0.4	7.1
MRL-*n*	No	*l*	7	—	—	—	−5±3	8.9±0.9	1.3
MRL-*n*	No	*n*	3–6	−25±3	7.4±0.2	0.26	—	—	—
MRL-*n*	Yes	*n*	8	−31±2	7.3±0.5	3.6	—	—	—
MRL-*l*	Yes	*n*	6	−30±3	5.3±0.7	2.2	—	—	—
C57, CBA	Yes	*n*	10	−30±3	6.0±0.3	1.8	—	—	—
BALB/c	Yes	*n*	4	−24±2	7.2+0.5	5.8	—	—	—
MRL-*l*	No	"bi"	8	−37±2	5.2±0.5	0.27	2±4	8.7±0.6	4.1
MRL-*n*	No	"bi"	3	−41±1	4.5±0.2	0.15	1±6	8.1±2.0	1.3

Means ± SE are given, with the number of cells (*n*). Cells were classified on the basis of kinetics or TEA sensitivity as mainly type *l* or type *n*. The parameters are defined in Eqs. 1 and 2. Cells with bimodal g_K-V relations ("bi") were fitted as described in the text to the sum of two Boltzmanns (Eq. 2). The type *n* component, while clearly present in some "bimodal" cells, was very small and only approximately quantified. "C57, CBA" includes nine C57BL/6J and one CBA/J cell.

resemble the actual data in many "bimodal" cells. These simulations show, in addition, that if the g_K-V curve in a cell with both types of channels is fitted with a single Boltzmann (Eq. 1), then the apparent slope will be more gradual than that of the predominant channel, and the apparent midpoint of the g_K-V relation will lie between the two fundamental values. Both of these effects can be seen in Table I, when parameters from bimodal fits are compared with those from single-component fits.

If this interpretation of two populations of K^+ channels in individual cells is correct, then the fraction of $g_{K,max}$ displaying type *n* voltage dependence in a cell with a bimodal g_K-V relation should be similar to the fraction of $g_{K,max}$ that is TEA resistant. In 12 cells in which both parameters were estimated, the fractions of g_K corresponding to type *n* TEA sensitivity and type *n* voltage dependence

were in reasonably good agreement, with a correlation coefficient $r = 0.95$ (data not shown).

K^+ Channel Activation and Closing Kinetics

The increase of K^+ current with time during a depolarizing voltage pulse occurs with a distinct delay in type *n* cells. This delay could be fitted tolerably well by Hodgkin-Huxley (1952) n^4 kinetics, as was found for K^+ currents in human T lymphocytes (Cahalan et al., 1985). Type *l* channels, on the other hand, appear to activate with less delay, and in some cells the activation kinetics appear to be almost exponential. Although exponential activation kinetics were reported for K^+ currents in murine clonal cytotoxic T lymphocytes (Fukushima et al., 1984), in most other respects the K^+ channels in these clonal cells resemble type *n* channels.

TABLE II

Hodgkin-Huxley Analysis of Type n K^+ Channel Kinetics in T Cells

Strain	Con A	*n*	$\bar{\alpha}_n$	$k_{\alpha,n}$	$\bar{\beta}_n$	$k_{\beta,n}$	$\bar{V}_n$
	h		s^{-1}	*mV*	s^{-1}	*mV*	*mV*
MRL-*n*	16–54	4	11±0.9	2.6±0.2	2.5±0.2	27.5±1.0	−42±3
MRL-*n*	—*	1	9	3	3.3	26	−36
MRL-*l*	24–47‡	5	12±2.4	2.5±0.1	2.5±0.3	27.8±1.7	−36±3
C57BL/6J	17–54	4	9.9±1.6	2.6±0.2	1.8±0.1	25.8±0.9	−37±4
Human	—	9	12±0.6	3.2±0.3	4.1±0.3	34±1.3	−38±2

Parameters were obtained by fitting the $1/\tau_n$ vs. voltage relation with the standard Hodgkin-Huxley (1952) n^4 model, as described in Cahalan et al. (1985). Means ± SE are given, with the number of cells (*n*). The rate constants were corrected for small differences in room temperature by individually scaling to 22.0°C, assuming a Q_{10} of 3.0. The values for human peripheral T lymphocytes were taken from Cahalan et al. (1985). The values for $\bar{\beta}_n$ and $k_{\beta,n}$ in human T cells differ significantly from the corresponding parameters in Con A–activated T cells from all three strains ($p < 0.05$ for each).

* A large (9 μm diam) cell from an unstimulated population, presumed to be spontaneously activated (see DeCoursey et al., 1987).

‡ These MRL-*l* T cells had been treated with Con A and were selected because they had enlarged. The K^+ channels in these cells (three from mice ≥4 mo old, two from 1.5-mo-old mice) were judged to be predominantly type *n* on the basis of TEA sensitivity (see also Chandy et al., 1986).

Since K^+ channel opening in type *n* cells could be described by n^4 kinetics, the activation and deactivation kinetics could be expressed in terms of the Hodgkin-Huxley (1952) model, for comparison with K^+ currents in other cells. Table II summarizes the parameter values for type *n* currents in Con A–activated MRL-*n*, C67BL/6J, and MRL-*l* cells, and also in a large, unstimulated MRL-*n* cell, along with values from unstimulated human T cells for comparison. All cells expressing type *n* channels have similar kinetic parameters. K^+ channels in human T cells may close slightly faster (greater $\bar{\beta}_n$), and with a slightly less steep voltage dependence (greater $k_{\beta,n}$), compared with murine type *n* K^+ channels, but these are subtle differences. Type *l* current activation was fitted too poorly by n^4 kinetics to allow similar analysis.

The mean time-to-half-peak K^+ current, $t_{1/2}$, in type *l* and in type *n* cells is plotted against potential in Fig. 3. Subtle but consistent differences in the voltage

dependence of $t_{1/2}$ are present. In many MRL-*l* cells, $t_{1/2}$ attained a maximum near −20 mV. In type *n* cells, $t_{1/2}$ always increased monotonically at more negative membrane potentials, as was previously observed for human T cells (Cahalan et al., 1985). The non-monotonic voltage dependence in some MRL-*l* cells is consistent with the existence of two populations of K^+ channels, the larger proportion of which have activation kinetics shifted to more positive potentials. Alternatively, type *l* channels may display a qualitatively different voltage dependence than type *n* channels.

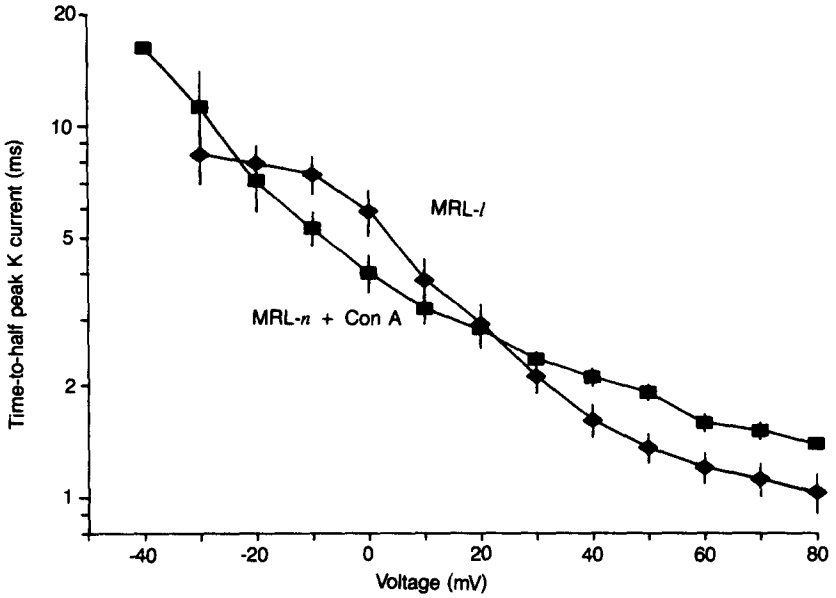

FIGURE 3. Voltage dependence of K^+ current activation kinetics. The mean (± SE) time-to-half-peak K^+ current is plotted for 6–13 MRL-*l* T lymphocytes (◆), and 3–4 Con A–activated MRL-*n* T lymphocytes (■, two cells only at −40 and + 80 mV). The time after a depolarizing voltage step for the K^+ current to reach half of its maximal value was determined after subtraction of a leak current estimated by linear extrapolation of the current recorded during subthreshold depolarizing pulses. Small variations in temperature were corrected to 23°C, assuming a Q_{10} of 3.0. The mean temperature before correction was 21.2°C in MRL-*l*, and 23.2°C in Con A–activated MRL-*n* cells. The difference in the voltage dependence of K^+ current kinetics around the threshold for activating g_K was apparent in individual cells.

The kinetics of K^+ channel closing, reflected by "tail currents," were strikingly different for the two types of channels. Type *n* tail currents in a Con A–activated MRL-*n* cell are illustrated in Fig. 4*A*. Type *l* tail currents, shown in an MRL-*l* cell in Fig. 4*B*, are much more rapid. Both types of K^+ channels close more rapidly at more negative potentials. The mean tail current time constants, τ_{tail}, are plotted in Fig. 5 for Con A–activated T cells from MRL-*n*, C57BL/6J, and CBA/J mice. Cells from all three strains exhibited very similar type *n* tail current

kinetics. The rate of K^+ channel closing is more than an order of magnitude faster in type *l* cells. In resting MRL-*n* cells classified as type *l*, τ_{tail} was indistinguishable from that in MRL-*l* cells, which supports the identity of type *l* channels in both strains. Compared in the middle of the voltage range studied, where the data are most reliable, τ_{tail} depends more steeply upon voltage in type *l* than in

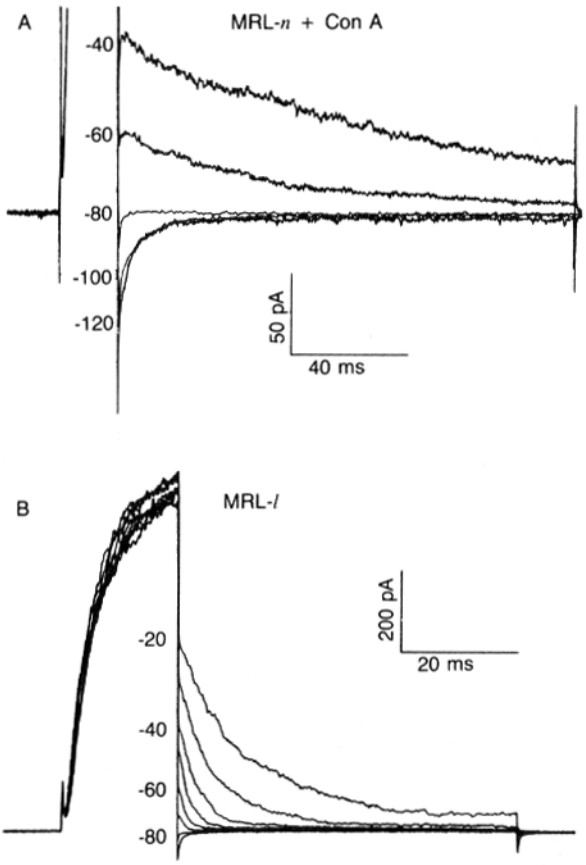

FIGURE 4. Tail current kinetics. The time course of the currents during each test pulse reflects the rate of K^+ channel closing at that potential. (*A*) Type *n* tail currents in a 16-h Con A–activated MRL-*n* cell. The cell was held at −80 mV, stepped briefly to +20 mV to open most K^+ channels, and then stepped to the potentials indicated. An interval of 20 s was allowed between pulses. The current during the prepulse is off the scale. (*B*) Type *l* tail currents in an MRL-*l* splenic T cell. The cell was held at −80 mV and pulsed to +20 mV with a 10-s interval. Note different time calibration from *A*.

type *n* cells. In type *l* cells, τ_{tail} changed e-fold every 16–20 mV, while in type *n* cells, it changed e-fold every 26–30 mV ($k_{\beta,n}$ in Table II).

Inactivation of K^+ Channels

One characteristic of delayed rectifier K^+ currents in a variety of cells, including skeletal muscle, nerve cell bodies, and various cells of the immune system, is that

recovery from inactivation is much slower than the onset of inactivation during maintained depolarization (Nakajima, 1966; Argibay and Hutter, 1973; Kostyuk et al., 1975; Aldrich et al., 1979; DeCoursey et al., 1984*a*; Ypey and Clapham, 1984; Fukushima et al., 1984; Cahalan et al., 1985; Gallin and Sheehy, 1985). This property is manifested operationally as an accumulation of inactivation during repeated depolarizing voltage steps. Fig. 6*A* illustrates the profound accumulation of inactivation typical of type *n* K^+ channels, during a train of brief depolarizing pulses repeated at ~1 Hz in a Con A–activated MRL-*n* cell. In contrast, type *l* K^+ channels exhibited almost no accumulation of inactivation. Fig. 6*B* shows that in an MRL-*l* cell, the K^+ current elicited by the 20th pulse is

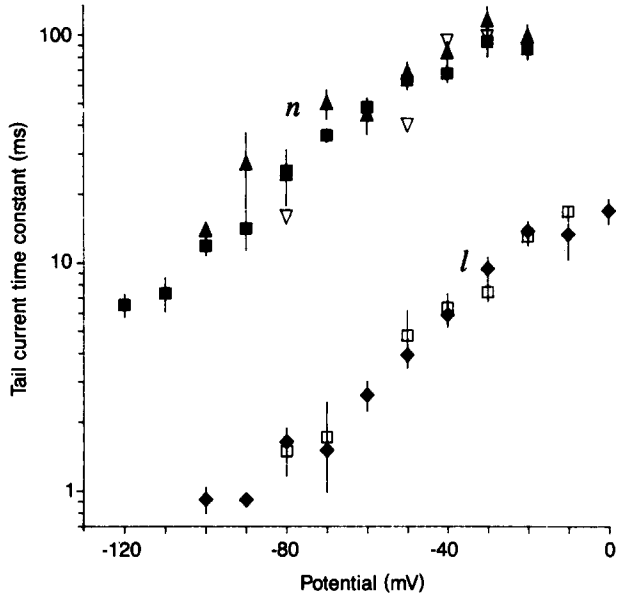

FIGURE 5. Mean (± SE) tail current time constants, τ_{tail}, obtained by fitting currents like those in Fig. 4 to a single exponential by adjusting the amplitude, time constant, and steady state current. Type *n* kinetics are illustrated in Con A–activated MRL-*n* cells (activated for 16–54 h by Con A, ■, n = 2–8 cells), in C57BL/6J cells (activated for 4–54 h, ▲, n = 3–7), and in two CBA/J cells (activated for 21–22 h, ▽). Type *l* kinetics are seen in MRL-*l* cells (◆, n = 3–15) and in unstimulated MRL-*n* cells judged, e.g., by high TEA sensitivity, to be mainly type *l* (□, n = 3–6).

at most only slightly smaller than that elicited by the 1st pulse in a pulse train similar to that in Fig. 6*A*.

Both types of K^+ currents inactivate under maintained depolarization in an approximately exponential manner (Fig. 6, *C* and *D*). In both types of cells, the rate and completeness of inactivation during maintained depolarization, as well as the extent of accumulation of inactivation in type *n* cells, increased during the first 10–20 min after the transition to the whole-cell configuration (cf. Cahalan et al., 1985). After equilibration, type *l* channels (Fig. 6*D*) inactivated more slowly and apparently less completely than type *n* (Fig. 6*C*). The mean time constants are plotted in Fig. 7. The inactivation rate of K^+ currents in MRL-*l*

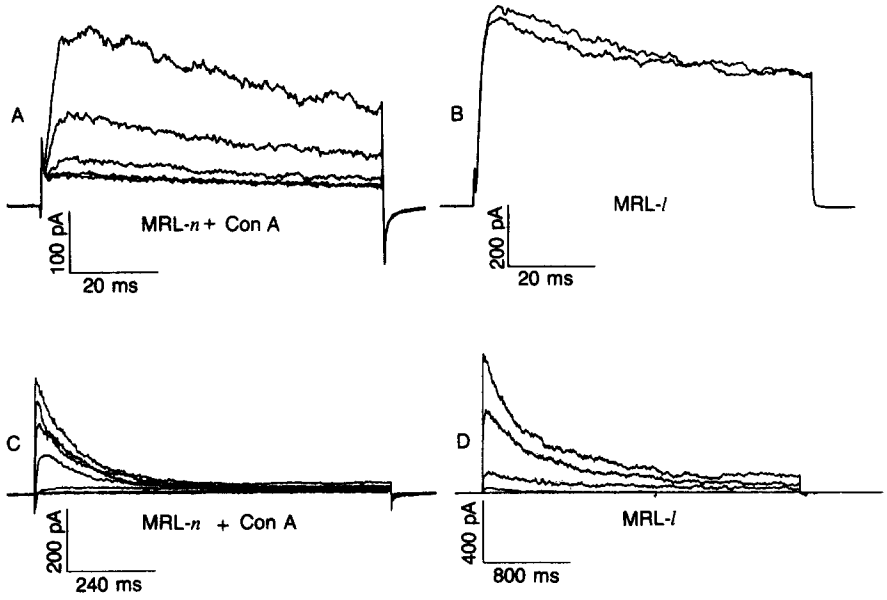

FIGURE 6. Inactivation of K^+ currents. Comparison of the kinetics of inactivation and recovery in type *n* cells (*A* and *C*) and in type *l* cells (*B* and *D*). (*A*) Accumulation of K^+ conductance inactivation in an MRL-*n* T lymphocyte after 54 h incubation with Con A. The cell was held at −80 mV for at least 80 s, and then 80-ms depolarizing pulses to +40 mV were applied at 1 Hz. Whole-cell currents during the first five pulses are shown, the first current being largest. Recorded 41 min after the whole-cell configuration was achieved. (*B*) Only a slight accumulation of inactivation is apparent in currents recorded in this MRL-*l* T lymphocyte, during a pulse train similar to that in *A*. The 1st and 20th currents are shown, the 1st being larger. This cell was held at −80 mV for at least 70 s, and then 80-ms pulses to +40 mV were applied at ~0.8 Hz. Recorded 15 min after achieving the whole-cell configuration. (*C*) Inactivation of K^+ currents during long depolarizing pulses in the Con A–activated MRL-*n* T lymphocyte shown in *A*. Depolarizing pulses 1 s in duration were applied at 30-s intervals, from a holding potential of −100 mV, in 20-mV increments up to +40 mV. Transient inward currents reflect the Na^+ channels present in this cell (see DeCoursey et al., 1987). Recorded 19 min after achieving the whole-cell configuration. (*D*) Inactivation of K^+ currents in an MRL-*l* T lymphocyte. Depolarizing pulses 3 s in duration were applied at 30-s intervals, from a holding potential of −80 mV, in 20-mV increments up to +40 mV. Recorded 22 min after the transition to the whole-cell configuration. Note different time calibration from *C*.

cells was indistinguishable from that in type *l* MRL-*n* cells. The inactivation time constant in type *l* channels was not perceptibly voltage dependent, and averaged 300–400 ms. Type *n* inactivation kinetics are practically independent of voltage at positive potentials, with a time constant averaging ~100 ms, but are clearly slower at negative potentials. In Con A–activated cells judged to be type *n* from MRL-*n*, CBA/J, and C57BL/6J mice, the time constant of inactivation was

virtually identical among the three strains. The voltage dependence of inactivation in type *n* channels is similar to that of K^+ channels in human T cells (Calahan et al., 1985), although inactivation appears to be slightly faster in murine T cells (Table III).

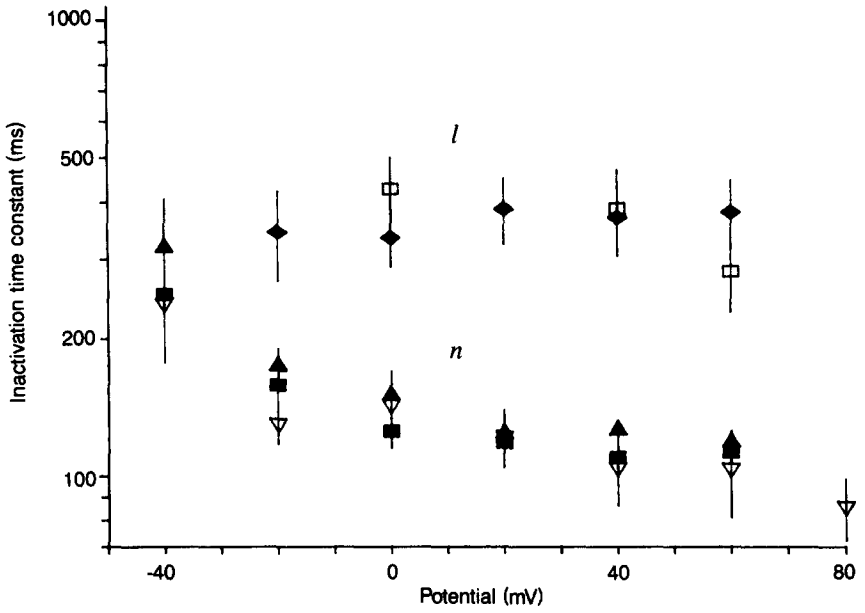

FIGURE 7. Time constants (mean ± SE) of K^+ current inactivation during depolarizing voltage steps. Type *n* behavior is seen in MRL-*n* cells activated by Con A for 16–54 h (■, n = 5–7 cells), in CBA/J cells activated for 21–24 h by Con A (▽, n = 3–4), and in C57BL/6J cells activated for 15–54 h by Con A (▲, n = 2–6). Type *l* behavior is seen in MRL-*l* cells (◆, n = 6–8) and in type *l* MRL-*n* cells (□, n = 3). Time constants were obtained by fitting whole-cell currents recorded during long depolarizing pulses, as in Fig. 6, *C* and *D*, to a single exponential: $I(t) = A \exp(-t/\tau_j) + C$, by adjusting the amplitude of the transient, A, the time constant τ_j, and the steady state current level, C.

The voltage dependence of steady state inactivation of the g_K was studied by varying the holding potential, V_{hold}, and recording the K^+ current, I_K, during pulses to a constant test potential. As shown in Fig. 8, the data could be fitted with a Boltzmann function:

$$I_K(V_{hold}) = \frac{I_{K,max}}{1 + \exp[(V_{hold} - V_j)/k_j]}, \quad (3)$$

where $I_{K,max}$ is the largest I_K available at any V_{hold}, V_j is the potential at which half the channels are inactivated, and k_j gives the steepness of the voltage dependence. The parameter values in Table III show that half the channels are inactivated at −62 mV and at −68 mV in type *l* and type *n* cells, respectively. These values are

not significantly different ($p > 0.1$). The steepness of the voltage dependence, k_j, is also similar in type *l* and type *n* cells.

Polyvalent Cation Effects

A surprising characteristic of the K^+ channels in human T lymphocytes is their sensitivity to block by agents, including polyvalent cations and organic compounds (DeCoursey et al., 1984*b*, 1985*c*), traditionally thought of as Ca^{++} channel blockers. To see whether murine K^+ channels share this sensitivity, we tested

TABLE III

K^+ Conductance and K^+ Channel Parameters in T Lymphocytes of Mice and Men

	Type *n*	Type *l*	Human
$g_{K,max}$ (nS)	0.37±0.10 (38)	4.6±0.6 (31)	4.17±0.22 (90)
V_n (mV)	−36±1.8 (8)	−9±2.2 (18)	−36±1.5 (28)
k_n (mV)	−7.3±0.5 (8)	−9±0.3 (18)	−4.3±0.6 (4)
V_j (mV)	−68±2 (3)	−62±3 (7)	−68±5 (4)
k_j (mV)	8.3±1.0 (3)	8.9±0.5 (7)	8.3±1.5 (4)
τ_{tail}, −60 mV (ms)	49±4 (6)	2.6±0.4 (13)	123
$k_{\beta,n}$ (mV)	26–30	16–20	34±1.3 (9)
τ_j (+40 mV)	107±6 (9)	340±44 (10)	178±13 (10)
Recovery	Slow	Fast	Slow
K_i for TEA (mM)	10–13	0.08	8
K_i for Co^{++} (mM)	2–5	>20	<0.5
Unit conductance (pS)	12	21	16, 9

All $g_{K,max}$ values are from unstimulated T cells of normal size (i.e., <8 μm diam) from MRL-*n* mice, MRL-*l* mice, or humans, respectively. All other parameters for type *n* channels are mainly from Con A–activated MRL-*n* cells, parameters for type *l* channels are from MRL-*l* cells, and the parameters for human T cells were taken from Cahalan et al. (1985) and DeCoursey et al. (1984*a*), except the K_i values for Co^{++} and τ_j, which are unpublished. All data were obtained at similar temperatures (20–24°C). The means ± SE are given, with the numbers of cells in parentheses. The parameters V_n and V_j were corrected for a −4.5-mV junction potential between KF and Ringer for murine T cells; for human T cells, they were recalculated from Cahalan et al. (1985) using the same junction potential correction. The tail current time constant, τ_{tail}, was calculated from Table 5 of Cahalan et al. (1985); $k_{\beta,n}$, which essentially reflects the slope of the τ_{tail}-V relation, was obtained from the fits described in Table II or directly from plots of τ_{tail}-V. Activation parameters V_n and k_n are defined in Eq. 1; inactivation parameters V_j and k_j are defined in Eq. 3. The time constant of inactivation, τ_j, was determined as in Fig. 7. "Recovery" refers to the rate of recovery from inactivation, which is manifested as the presence or absence of cumulative inactivation during repeated depolarizing pulses. For blockers, K_i is the concentration at which the (leak-subtracted) K^+ current during a depolarizing step is reduced to one-half.

Co^{++} and La^{+++}, because at low concentrations these cations had profound effects on K^+ currents in human T cells. Fig. 9*A* shows that 5 mM Co^{++} added to Ringer reduced the K^+ current at +40 mV by >50% in a Con A–activated MRL-*n* cell. In two type *n* cells (MRL-*n* activated with Con A), 100 μM La^{+++} reduced $g_{K,max}$ to 40% of its value in Ringer. Type *n* K^+ channels in murine cells thus share with human T cells the property of being blocked by polyvalent cations, although they may be somewhat less sensitive (Table III). In contrast, type *l* channels were practically insensitive to block by Co^{++}. Fig. 9*B* shows the effect of 20 mM Co^{++} on the g_K-V relation of an MRL-*l* cell, compared with before and after measure-

ments made in Ringer in the same cell. The saturating level of g_K is reduced to 0.83, normalized to the mean of the before and after values in Ringer to correct for rundown. Table IV summarizes the effect of Co^{++} and Ca^{++} on type *l* K^+ channels. The average reduction of $g_{K,max}$ by 20 mM Co^{++} was only 10%. Table IV also shows that the $g_{K,max}$ in type *l* cells was insensitive to block by external Ca^{++}. No block was detected even with 120 mM Ca^{++} in one MRL-*l* cell. In contrast, 100 mM Ca^{++} reduced $g_{K,max}$ substantially in human T cells (unpublished), presumably by a blocking mechanism similar to that of Co^{++}, La^{+++}, and other polyvalent cations (DeCoursey et al., 1985*c*). In general, type *l* K^+ channels

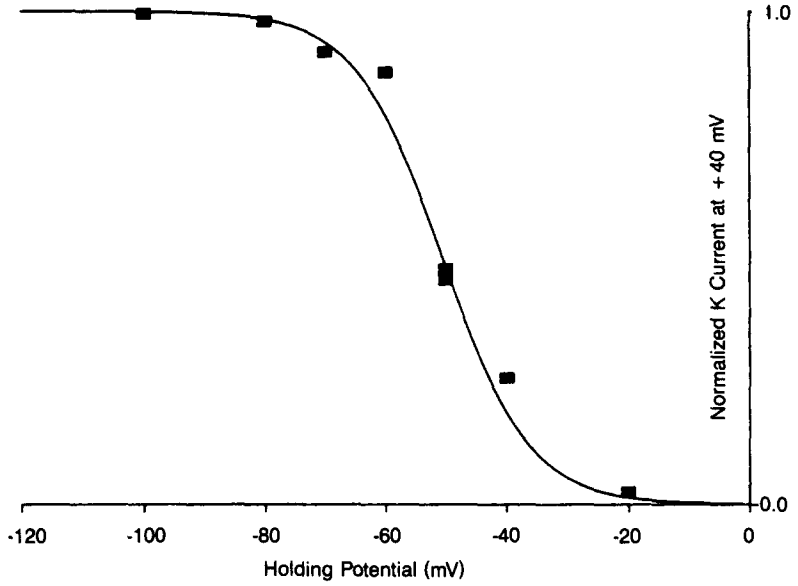

FIGURE 8. Voltage dependence of steady state inactivation of g_K in an MRL-*l* cell. The membrane potential was clamped to the potentials on the abscissa, and brief (40-ms) test pulses to +40 mV were applied every 30 s until the level of inactivation appeared to attain a steady state. Peak K^+ currents during the test pulse, after leak subtraction, were fitted to Eq. 3 (text) and then normalized to the fitted maximum. The fitted midpoint, V_j, was -49.8 ± 1.1 mV ($\pm$ SD in the fit) with a slope factor, k_j, of 7.2 ± 1.2 mV.

are less sensitive to block by polyvalent cations than are type *n* K^+ channels in mice or K^+ channels in human T cells.

One clear effect of polyvalent cations on type *l* K^+ channels is apparent in Fig. 9*B*. In this cell, the g_K-*V* relation was reversibly shifted +37 mV by 20 mM Co^{++}, with no change in the steepness of the voltage dependence. Voltage shifts resulting from changes in polyvalent cation concentrations, first observed by Frankenhaeuser and Hodgkin (1957), are well known for delayed rectifier K^+ channels in nerve (Hille, 1968). These effects are usually attributed to screening of, or binding to, negatively charged groups on the external face of the mem-

brane. If polyvalent cations of equal charge shift a parameter to a different extent, this is taken as evidence for specific binding, since, without binding, all cations of a given valence should be equally effective. The effects of Ca^{++} and Co^{++} on the g_K-V and $t_{½}$-V relations are summarized in Table IV. The shifts in both the g_K-V and $t_{½}$-V relations are greater for Co^{++} than for Ca^{++}, which suggests that specific binding sites are involved. It is also apparent from Table IV that the shifts of the activation kinetics ($t_{½}$-V) are greater than those for the g_K-V relation. This difference is significant for the 20 mM Co^{++} data ($p < 0.01$); in seven of eight experiments with Co^{++} or Ca^{++} in which both shifts were estimated, the shift in $t_{½}$-V was greater than the shift in g_K-V. In one cell, the voltage dependence of K^+ channel deactivation, τ_{tail}-V, was shifted reversibly by

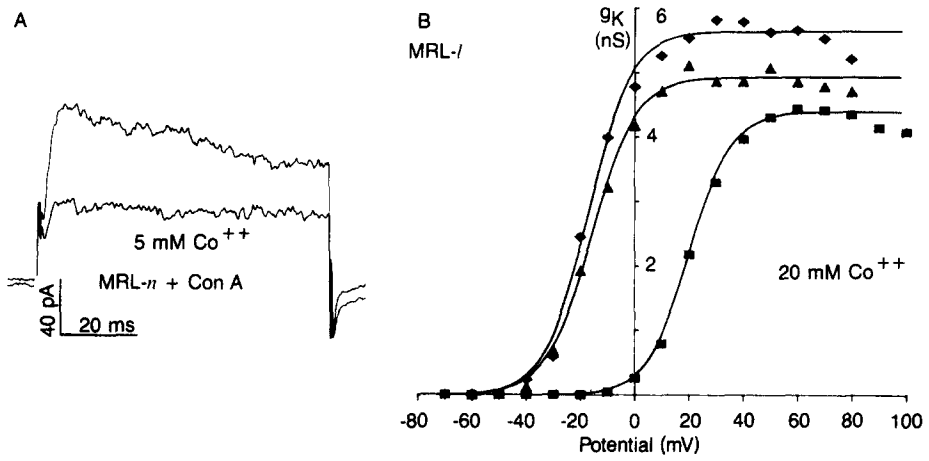

FIGURE 9. Effects of Co^{++} on type l and type n K^+ channels. (*A*) Block of type n K^+ currents in a Con A–activated MRL-n cell by 5 mM Co^{++} added to Ringer. This cell was held at −80 mV and stepped to +40 mV. (*B*) Effects of 20 mM Co^{++} on the peak g_K-V relation in an MRL-l T cell. The conditions were similar to those described in Fig. 2. Measurements were made in Ringer (◆), then with 20 mM Co^{++} added (■), and again in Ringer after washout of Co^{++} (▲). The smooth curves show the fit of these data to Eq. 1 with parameter values for before, with Co^{++}, and after, respectively: midpoint V_n, −16.5, +20.9, and −15.3 mV; slope factor k_n, −8.0, −7.8, and −8.3; and $g_{K,max}$, 5.65, 4.40, and 4.94 nS.

about +24 mV by 20 mM Co^{++}, clearly a smaller shift than for g_K-V or $t_{½}$-V in that cell or in all the cells in Table IV. Gilly and Armstrong (1982) observed a similar phenomenon in squid giant axon, namely that the voltage dependence of K^+ current activation was shifted by polyvalent cations more than that of deactivation, with an intermediate shift in g_K-V.

Effects of Other K^+ Channel Blockers

A variety of pharmacological agents known to block K^+ channels in human T lymphocytes (DeCoursey et al., 1984*a*, *b*, 1985*c*; Chandy et al., 1984, 1985) also block K^+ channels in murine T cells. Both types of K^+ channels were blocked by 4-AP, with half-block at concentrations <200 μM. Type l K^+ channels (classified

in each cell by high sensitivity to external TEA) were also blocked by quinine, verapamil, nifedipine, cetiedil, and diltiazem, with 50% reduction of the peak K^+ current occurring in the range of 4–40 μM. Type *n* K^+ channels were blocked by these compounds at roughly similar concentrations. All of these agents increased the apparent rate of K^+ current inactivation, and in some cases produced "use-dependent" block; both results suggest that the block is state dependent (cf. DeCoursey et al., 1984*b*, 1985*c*). Because of the complex nature of the block, the apparent blocking potency depends on the way it is measured, and quantitative comparison of dose-response curves for the two types of K^+ channels is somewhat arbitrary.

TABLE IV

Divalent Cation Effects on Type l K^+ Channels

Cation (X^{++})	Δg_K-V	n	$\Delta t_{1/4}$-V	n	$\Delta g_K(X^{++})/g_K$
	mV		*mV*		
"0" mM Ca^{++}	−14	1	—	—	>0.8
20 mM Ca^{++}	+14.3±2.1	3	+16	2	1.06
5 mM Co^{++}	+18.9	2	+27.5	2	0.94
20 mM Co^{++}	+35.9±2.2	5	+47.5±1.7	4	0.90

Mean (± SE) shifts, for the number of cells (*n*), are relative to the voltage dependence in normal Ringer (containing 2 mM Ca^{++} and 1 mM Mg^{++}). The shift in the g_K-V relation was determined as shown in Fig. 9*B*. The shift in $t_{1/4}$-V was determined by plotting the $t_{1/4}$-V relations as in Fig. 3 and estimating the shift by eye. For both parameters, the value for the shift was taken as the mean shift relative to the data in Ringer before and after exposure to the altered divalent cation concentration, to correct for slow drift. The effect of X^{++} on the maximum g_K, $g_K(X^{++})/g_K$, was determined as illustrated in Fig. 9*B*, from the saturating level of g_K at positive voltages, again taking the mean of measurements in Ringer before and after exposure to X^{++} to correct for rundown. In the "0" mM Ca^{++} experiment, Ringer without added Ca^{++} (or Ca^{++} buffers) was used. The value for $g_K(X^{++})/g_K$ in this experiment is underestimated because a large increase in leak current suddenly occurred before measurements of the g_K-V relation were completed; upon return to Ringer, the leak decreased to a low value.

Single K^+ Channel Currents

Single K^+ channel currents were studied in cells with few channels by using voltage pulses or ramps in the whole-cell configuration. In cells with many channels, such as MRL-*l* cells or Con A–activated cells, unitary currents were observed by holding the cell at a fairly positive potential, thereby allowing the inactivation process to reduce the number of open channels to a low level, or by studying channels in outside-out patches of membrane. The single channel measurements summarized in Table V revealed that two distinct sizes of K^+ currents are present in MRL mouse T lymphocytes, with properties that correlate well with the behavior of macroscopic K^+ currents. A third class of "tiny" unitary currents was observed infrequently; their relationship to macroscopic currents is unclear.

In MRL-*l* cells with macroscopically identified type *l* channels, the unitary currents were fairly uniform in amplitude, corresponding to a mean conductance

of 21 pS (Table V, "large"). MRL-*n* cells could be classified either as type *l* or type *n* on the basis of macroscopic g_K behavior. Three cells classified as type *l* expressed large events similar in size to channels in MRL-*l* cells, while four cells classed as type *n* expressed a smaller maximum unitary conductance (~12 pS; Table V, "small"). These results suggest that the larger 21-pS channels underlie type *l* macroscopic behavior, and that the smaller 12-pS channels underlie type *n* macroscopic behavior. Pharmacological evidence supports this interpretation. "Large" channels in MRL-*l* cells were blocked potently by TEA, as shown in Fig. 10*B*. "Small" channels in type *n* MRL-*n* cells were blocked only by much higher concentrations of TEA, as shown in Fig. 10*A*. Block of both types of channels was manifested as a reduction in the apparent single channel current amplitude.

TABLE V

Unitary K^+ Channel Conductances in Mouse T Cells

Strain	Large	Small	Tiny
	pS	*pS*	*pS*
MRL-*l*	20.5±0.9 (8)	11.3 (2)	—
MRL-*n*	20.6±0.9 (8)	11.9±0.7 (3)	—
MRL-*n*	—	12.2±0.4 (8)	7.3±0.5 (3)
CBA/J	18.4±0.6 (3)	9.8±0.4 (3)	—
C57BL/6J	23.6 (1)	13.6 (2)	6.0 (1)
C3H/HeJ	—	9.3 (1)	—

Means ± SE are given, with the numbers of cells in parentheses. Unitary conductances, estimated by averaged ramp-clamp data or by measuring unitary current amplitudes at several potentials, are grouped into three categories. Including data from all strains, the range of values for each category is: large, 16–24 pS; small, 9–14 pS; and tiny, 6–8 pS. For MRL-*n* cells, the first line gives values from cells in which the largest events were within the range classified as "large" (presumably type *l*), and the second line gives values from cells in which the largest events were "small" (presumably type *n*). For CBA/J cells, two conductance levels were seen in each cell; for C57BL/6J, only one amplitude was seen in each cell. Unitary conductances were determined either by measuring unitary currents at various potentials, or by averaging ramp-clamp events, as in the examples in Fig. 10.

The simplest interpretation of these data is that two distinct types of K^+ channels are present in MRL T cells, a 21-pS type *l* channel and a 12-pS type *n* channel.

The single K^+ channel conductances in T cells from several other strains of mice are included in Table V. The unitary conductances are classified according to size, by analogy with MRL. All three CBA/J cells studied clearly expressed both large and small unitary currents. In four C57BL/6J cells, only one size of unitary current could be distinguished with confidence in each cell, but the current amplitudes fell into all three of the categories established for MRL. Although the apparent similarity of the unitary conductances in resting cells from different strains could be coincidental, the simplest interpretation is that type *l* and type *n* K^+ channels have similar properties in all mouse strains.

Both Types of K^+ Channels Can Coexist in the Same Cell

For the biological interpretation of K^+ channel expression in certain populations of cells (see DeCoursey et al., 1987), it is of interest to know whether both types

of channels are ever present in the same cell, or whether they occur only in mutually exclusive subsets of cells. While macroscopic measurements in some instances suggest that both types of channels might coexist in the same cell (bimodal g_K-V and TEA dose-response curves), this suggestion was not completely satisfying, because one channel type almost invariably predominated, accounting for 80–90% of the total g_K, so that the other channel type could not be distinguished with confidence from "noise" in the data. Analysis of single K^+ channel currents, summarized in Table V, suggests that both types of channels can indeed coexist in the same cell. In many MRL-*n* cells with large maximum unitary conductances, smaller events also were observable, with a mean conductance of 11.9 pS. In some MRL-*n* cells, the 21-pS (type *l*) channel was never seen, and the largest events averaged 12.2 pS. "Small" events of similar amplitude, 11.3 pS, were also seen in a few (two of eight) MRL-*l* T cells, although infrequently. The similarity of these unitary conductances suggests that the same type *n* channel is present in all cases. Thus, both "large" and "small" unitary K^+ currents were observed frequently in individual cells, which supports the coexistence of *l* and *n* channel types.

Two pieces of evidence suggest that the large and small events in MRL-*n* cells reflect the presence of type *l* and type *n* K^+ channels in the same cell, rather than, for example, two substates of the same channel. First, Fig. 10*C* illustrates averaged unitary i_K-V (single K^+ channel current-voltage) curves for selected large and small events in a single MRL-*n* T cell. The cell was ramped repeatedly from −50 to +80 mV. Only one or two channels opened during most ramps, so that the two single channel current amplitudes could usually be distinguished. The voltage dependence of the two sizes of events was different. The larger-sized unitary events were observed in 57 of 60 ramps, first opening at an average potential of +4 ± 2 mV (SE). Smaller events were detected in 21 ramps, with a mean first opening potential of −18 ± 2 mV. Thus, the smaller-conductance channels appear to open at more negative potentials than the larger-conductance channels. Because the opening rates of K^+ channels are not instantaneous compared with the ramp rate (650 mV/s), the average potential at which channels first open is somewhat more positive than the "threshold" of macroscopic g_K-V curves. However, that the larger 21-pS channels first open at more positive potentials is consistent with their identification as underlying type *l* macroscopic currents that activate at more positive potentials; conversely, 12-pS channels reflect the voltage dependence of type *n* macroscopic K^+ currents.

Second, the presence of two distinct channel types in the same cell can be revealed by experiments like that illustrated in Fig. 10*D*. The larger i_K-V curve was obtained in Ringer solution in an MRL-*n* cell judged to be predominantly type *l* by macroscopic criteria. The predominant events in ramp-clamp records correspond to ~21 pS. Although no smaller events were clearly distinguished in the ramp records in Ringer, when unitary currents were recorded at different holding potentials (allowing most channels to inactivate), both large and small events were clearly detectable. The application of 5 mM TEA reduced the macroscopic outward current by >80%, which is consistent with the classification of the cell as predominantly type *l*. The predominant unitary conductance in the presence of 5 mM TEA, however, was ~10 pS (cf. the greater reduction of type

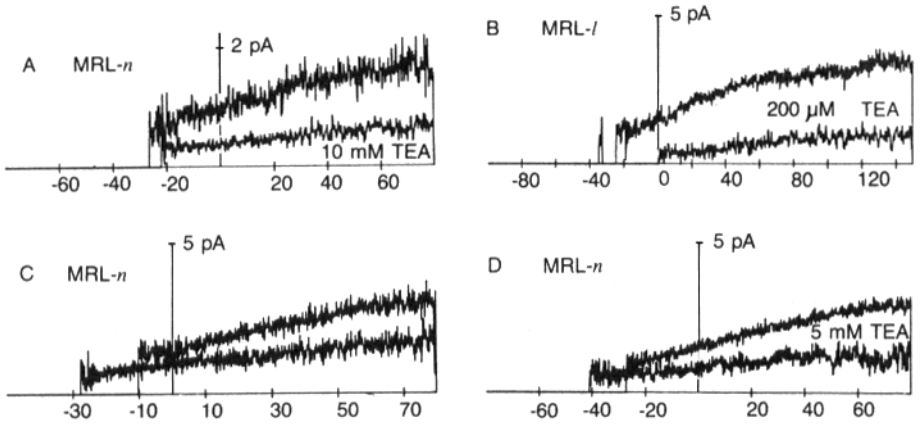

FIGURE 10. Average single K^+ channel current-voltage (i_K-V) relationships. For each, the command potential was ramped repeatedly (16–80 ramps) from the potential at the negative end of the abscissa to that at the positive end. The records were sorted off-line, with portions of current records judged to include no channel openings averaged to provide an average leak current. Similarly, portions of records judged to include currents through a single open channel were averaged and the averaged leak was subtracted, resulting in average unitary i_K-V relations. The range of the data is limited at negative potentials, partly because the unitary currents are smaller and hard to detect, but primarily because K^+ channels rarely open at negative potentials. (*A*) The larger trace represents averaged unitary type *n* channel currents; the smaller currents are from the same MRL-*n* cell in the presence of 10 mM TEA. Low-pass filter, 1 kHz. Larger events were selected; some distinctly smaller events were also present, but were excluded from the average. In the presence of TEA, it was not possible to distinguish between different-sized events, so some smaller events may be included in the average. In addition, brief closures were easier to exclude from the average in TEA-free Ringer; both factors tend to reduce the apparent conductance in the presence of TEA. Linear regression gives 11.2 pS and −99 mV for the unitary conductance and reversal potential, respectively, in Ringer, and 4.4 pS and −87 mV in the presence of TEA. (*B*) Averaged type *l* channel current recorded in an outside-out patch of membrane from an MRL-*l* cell. The larger current was recorded in Ringer; the smaller current was recorded in the presence of 200 μM TEA. Linear regression of the data negative to +70 mV gives 22.6 pS and −67 mV for Ringer, and 4.9 pS and −71 mV for TEA. Rectification of the unitary current-voltage relation at potentials positive to about +80 mV was observed regularly in type *l* channels; however, in many cells, the leak conductance was more variable and nonlinear at large positive potentials, reducing the reliability of the *i*-*V* relation in this region. Filter, 1 kHz. (*C*) Two sizes of K^+ channel currents in the same cell in Ringer. This MRL-*n* cell was classified as predominantly type *l* on the basis of macroscopic current behavior. The cell, which had a large g_K, was held at −50 mV to inactivate most of the K^+ channels and thus facilitate recording single channel currents. Large and small events were averaged separately; note that the smaller events were present at more negative potentials. Linear regression gives 22.1 pS and −69 mV for the larger (type *l*) currents and 11.9 pS and −80 mV for the smaller (type *n*) currents. The cell equilibrated at least 53 min after the transition to whole cell. Filter, 2 kHz. (*D*) Pharmacological evidence

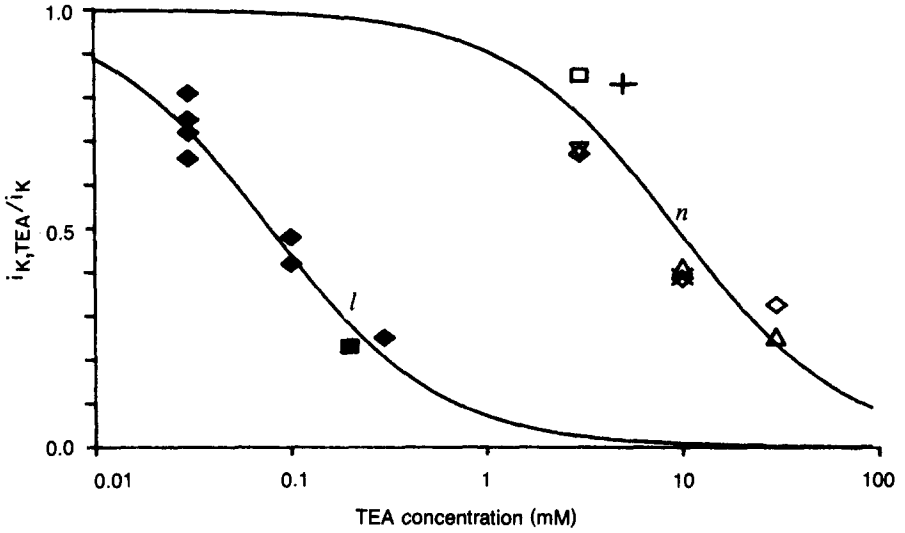

FIGURE 11. Dose-response relationships for the reduction of unitary K^+ channel current amplitude by externally applied TEA. Each data point shows the ratio of the average unitary current in the presence of the indicated concentration of TEA to that in its absence, measured using ramp clamps as described in Fig. 10. The smooth curves show the inhibition of current expected for K_i values of 80 μM and 10 mM. The filled symbols represent measurements in two outside-out patches of membrane from MRL-*l* cells expressing type *l* channels; the open symbols represent type *n* channels in six different MRL-*n* cells. Different symbols indicate different cells. In MRL-*n* cells in which both large and small events were present in Ringer, the smaller events were assumed to reflect type *n* channels; those events remaining in the presence of millimolar concentrations of TEA were assumed also to reflect type *n* channels (see text for full rationalization of these assumptions).

l channel current by 0.2 mM TEA in Fig. 10*B*). The simplest interpretation of this result is that TEA completely blocked all the type *l* channels in the cell, revealing the presence of a few type *n* channels, whose conductance was only slightly reduced by 5 mM TEA.

Fig. 11 shows dose-response relations for the reduction of the type *l* (filled symbols) and type *n* (open symbols) single K^+ channel current amplitude by

---

that both type *l* and type *n* channels can be present in the same cell. This MRL-*n* T cell was classified as mainly type *l* because the whole-cell peak K^+ current during a step to +40 mV was reduced substantially, from 27 to ~5 pA, by 5 mM TEA. The larger averaged unitary current was recorded in Ringer; the smaller current was recorded in the presence of 5 mM TEA. In the ramp records in Ringer, large events were predominant and no smaller events were clearly distinguished. In the presence of TEA, the unitary current amplitudes appeared variable; larger events were selected for averaging. Linear regression gives 21.1 pS and −73 mV in Ringer and 9.8 pS in TEA. Filter, 1.2 kHz.

external TEA. The smooth curves are drawn for half-block by 80 μM and 10 mM TEA, respectively. For both, the apparent reduction in the unitary current corresponds fairly well to the reduction of macroscopic K^+ currents by TEA in cells expressing predominantly one or the other type of channel (Fig. 1 *D*), which suggests that this effect of TEA is sufficient to account for the macroscopic block observed. For both channel types, the reduced single K^+ channel current amplitude may reflect a transient block with kinetics above the frequency range explored (1–2 kHz). Additional effects of TEA on single K^+ channel gating behavior are not ruled out.

DISCUSSION

Two Types of K^+ Channels in Murine T Lymphocytes

The properties of two types of voltage-gated K^+ channels in murine T lymphocytes are described in this article. These two K^+ channels have a number of superficial similarities. Both are activated by depolarization with roughly similar $t_{1/2}$ values, both display time-dependent inactivation during maintained depolarization and a similar steady state voltage dependence of inactivation, and both are blocked by TEA, 4-AP, quinine, and several organic "calcium antagonists." However, for virtually every parameter studied, quantitative differences between the two channel types were consistently observed. Some of these differences, in particular the TEA sensitivity, tail current kinetics, and rate of recovery from inactivation, were so striking as to be "diagnostic" for the categorization of the predominant channel type present in a given cell. The properties of these two channel types and, for comparison, of K^+ channels in human peripheral T lymphocytes are summarized in Table III. These descriptions are based primarily upon measurements in MRL-*l* T lymphocytes, which almost invariably express large numbers of type *l* channels, and in Con A–activated MRL-*n* T lymphocytes, which almost invariably express large numbers of type *n* channels. The behavior of type *n* K^+ channels in Con A–activated T cells from all strains of mice studied appears indistinguishable. Type *l* channels, compared with type *n*, activate at ~30 mV more positive potentials and with a less steep voltage dependence, have much faster tail current kinetics, inactivate more slowly and less completely while recovering from inactivation much more rapidly, have larger unitary conductances, are 100-fold more sensitive to block by external TEA, and are less sensitive to block by external Co^{++}.

Comparison of Murine K^+ Channels with K^+ Channels in Other Cells

Murine type *n* K^+ channels, like those in human T cells, closely resemble delayed rectifier K^+ channels in skeletal muscle and molluscan neurons, which in both preparations display slow and complex kinetics of recovery from inactivation (Adrian et al., 1970; Argibay and Hutter, 1973; Aldrich et al., 1979) and are blocked by 8 mM external TEA (see Stanfield, 1983). TEA reduces the apparent unitary delayed rectifier K^+ current in skeletal muscle membranes (Standen et al., 1985), in human peripheral T lymphocytes (unpublished), and in both type *n* and type *l* murine K^+ channels (Fig. 10), which in all cases probably reflects

blocking kinetics above the resolved frequency range. As pointed out previously (Cahalan et al., 1985), the only distinct difference between the voltage dependence or kinetics of K^+ channels in T lymphocytes and in skeletal muscle is that T cell (type *n*) K^+ channels close about an order of magnitude more slowly, i.e., the tail currents are slower. Marty and Neher (1985) described two types of voltage-gated K^+ channels in bovine chromaffin cells. The voltage dependence, activation kinetics, and unitary conductance (18 pS) of their "fast K" channels resemble type *n* K^+ channels in murine and human T lymphocytes. The weak voltage dependence of both the opening probability and the activation kinetics of their "slow K" channels appear to distinguish them from either type of K^+ channel in murine T cells.

One reason for considering type *n* channels to be "normal" is that their gating kinetics, voltage dependence, and pharmacology closely resemble the properties of K^+ channels in human peripheral blood T cells (DeCoursey et al., 1984*a*; Matteson and Deutsch, 1984; Cahalan et al., 1985), several human and murine T lymphocyte–derived cell lines (DeCoursey et al., 1985*c*), clonal murine cytotoxic T lymphocytes (Fukushima et al., 1984), clonal murine helper T lymphocytes (Lee et al., 1986), and cultured murine macrophages (Ypey and Clapham, 1984; Gallin and Sheehy, 1985). Type *l* K^+ channels are substantially different. In Tables II and III, the properties of the two types of murine K^+ channels are compared with those of K^+ channels in human peripheral T lymphocytes studied under similar conditions. While there are some quantitative differences, the kinetics and voltage dependence of activation and deactivation in murine type *n* K^+ channels are generally remarkably similar to those in human T cells. In human cells, despite the existence of two sizes of unitary K^+ conductance, there is no evidence for the presence of any type *l* channels; TEA dose-response curves and the voltage dependence of g_K indicate that there is one population of channels with type *n* behavior (DeCoursey et al., 1984*a*; Cahalan et al., 1985). The inactivation mechanism of type *n* K^+ currents in MRL T cells resembles that in human T cells, with respect to its kinetics of onset, steady state voltage dependence, and complex recovery kinetics. The slower time constant of inactivation of type *l* K^+ channels compared with type *n* or human K^+ channels (Table III) appears to be similar to the inactivation time constants in several other murine cell types: clonal cytotoxic T lymphocytes (Fukushima et al., 1984), macrophages (Ypey and Clapham, 1984), and a macrophage-derived cell line (Gallin and Sheehy, 1985). However, the presence of F^- in our pipette solution may invalidate this comparison with studies using Cl^- as the predominant anion in the pipette, since F^- accelerates the inactivation of K^+ currents in human T cells (Cahalan et al., 1985). In other respects, the K^+ channels in all of these cells resemble type *n* channels.

Table III shows that the pharmacological sensitivity of the type *n* K^+ channel in MRL T cells, compared with the type *l* channel, is clearly more similar to that of human T cells (DeCoursey et al., 1984*a*, *b*; Chandy et al., 1984). The half-blocking concentration of externally applied TEA for type *n* K^+ channels, ~8–16 mM, was slightly higher than that in human T cells (8 mM; DeCoursey et al., 1984*a*), but similar to that in murine clonal cytotoxic T lymphocytes (14 mM;

Fukushima et al., 1984). The high sensitivity of type *l* K^+ channels to TEA is perhaps their most striking characteristic. Being half-blocked by 50–100 μM external TEA, type *l* channels are among the most sensitive K^+ channels in a variety of preparations (Stanfield, 1983). Type *n* K^+ channels appear to be somewhat less sensitive to block by externally applied Co^{++} than are K^+ channels in human T cells (DeCoursey et al., 1984*b*; unpublished data), and type *l* channels are practically insensitive to block by Co^{++} or Ca^{++}. Collectively, these data demonstrate that despite certain quantitative differences, type *n* K^+ channels are closely similar to K^+ channels in human T cells and in murine clonal cytotoxic T lymphocytes or macrophages. Type *l* K^+ channels appear to represent a distinctly different channel type. Whether the type *l* channel is structurally different from type *n* channels, or whether these differences reflect modulatory effects of membrane or cytoplasmic constituents, remains to be determined.

In the following article (DeCoursey et al., 1987), we describe changes in the number of K^+ channels after stimulation by the mitogen Con A.

This work was supported by a Research Career Development Award (M.D.C.), by the American Diabetes Association, Southern California Affiliate (K.G.C.), and by U.S. Public Health Service grants NS-14609, AI-21808, AI-20717, and AG-04361.

Original version received 22 July 1985 and accepted version received 10 September 1986.

REFERENCES

Adrian, R. H., W. K. Chandler, and A. L. Hodgkin. 1970. Slow changes in potassium permeability in skeletal muscle. *Journal of Physiology.* 208:645–668.

Aldrich, R. W., P. Getting, and S. H. Thompson. 1979. Inactivation of delayed outward current in molluscan somata. *Journal of Physiology.* 291:507–530.

Altman, A., A. N. Theofilopoulos, R. Weiner, D. H. Katz, and F. J. Dixon. 1981. Analysis of T cell function in autoimmune murine strains: defects in production of and responsiveness to interleukin 2. *Journal of Experimental Medicine.* 154:791–808.

Argibay, J. A., and O. F. Hutter. 1973. Voltage-clamp experiments on the inactivation of the delayed potassium current in skeletal muscle fibres. *Journal of Physiology.* 232:41P–43P. (Abstr.)

Cahalan, M. D., K. G. Chandy, T. E. DeCoursey, and S. Gupta. 1985. A voltage-gated potassium channel in human T lymphocytes. *Journal of Physiology.* 358:197–237.

Chandy, K. G., T. E. DeCoursey, M. D. Cahalan, and S. Gupta. 1985. Electroimmunology: the physiologic role of ion channels in the immune system. *Journal of Immunology.* 135:787s–791s.

Chandy, K. G., T. E. DeCoursey, M. D. Cahalan, C. McLaughlin, and S. Gupta. 1984. Voltage-gated K channels are required for T lymphocyte activation. *Journal of Experimental Medicine.* 160:369–385.

Chandy, K. G., T. E. DeCoursey, M. Fischbach, N. Talal, M. D. Cahalan, and S. Gupta. 1986. Altered K^+ channel expression in abnormal T lymphocytes from mice with the *lpr* gene mutation. *Science.* 233:1197–1200.

DeCoursey, T. E., K. G. Chandy, S. Gupta, and M. D. Cahalan. 1984*a*. Voltage-gated K^+ channels in human T lymphocytes: a role in mitogenesis? *Nature.* 307:465–468.

DeCoursey, T. E., K. G. Chandy, S. Gupta, and M. D. Cahalan. 1984*b*. Pharmacology of human T lymphocyte K channels. *Biophysical Journal.* 45:144*a*. (Abstr.)

DeCoursey, T. E., K. G. Chandy, M. Fischbach, N. Talal, S. Gupta, and M. D. Cahalan. 1985*a*. Two types of K channels in T lymphocytes from MRL mice. *Biophysical Journal.* 47:387*a*. (Abstr.)

DeCoursey, T. E., K. G. Chandy, M. Fischbach, N. Talal, S. Gupta, and M. D. Cahalan. 1985*b*. Potassium channel expression in proliferating murine T lymphocytes. *Federation Proceedings.* 44:1310. (Abstr.)

DeCoursey, T. E., K. G. Chandy, S. Gupta, and M. D. Cahalan. 1985*c*. Voltage-dependent ion channels in T lymphocytes. *Journal of Neuroimmunology.* 10:71–95.

DeCoursey, T. E., K. G. Chandy, S. Gupta, and M. D. Cahalan. 1987. Mitogen induction of ion channels in murine T lymphocytes. *Journal of General Physiology.* 89:405–420.

Fernandez, J. M., A. P. Fox, and S. Krasne. 1984. Membrane patches and whole-cell membranes: a comparison of electrical properties in rat clonal pituitary (GH_3) cells. *Journal of Physiology.* 356:565–585.

Frankenhaeuser, B., and A. L. Hodgkin. 1957. The action of calcium on the electrical properties of squid axons. *Journal of Physiology.* 137:218–244.

Fukushima, Y., S. Hagiwara, and M. Henkart. 1984. Potassium current in clonal cytotoxic T lymphocytes from the mouse. *Journal of Physiology.* 351:645–656.

Gallin, E. K., and P. A. Sheehy. 1985. Differential expression of inward and outward potassium currents in the macrophage-like cell line J774.1. *Journal of Physiology.* 369:475–499.

Gilly, W. F., and C. M. Armstrong. 1982. Divalent cations and the activation kinetics of potassium channels in squid giant axons. *Journal of General Physiology.* 79:965–996.

Hille, B. 1968. Charges and potentials at the nerve surface. Divalent ions and pH. *Journal of General Physiology.* 51:221–236.

Hodgkin, A. L., and A. F. Huxley. 1952. A quantitative description of membrane current and its application to conduction and excitation in nerve. *Journal of Physiology.* 117:500–544.

Kostyuk, P. G., O. A.. Krishtal, and P. A. Doroshenko. 1975. Outward currents in isolated snail neurons. I. Inactivation kinetics. *Comparative Biochemistry and Physiology.* 51C:259–263.

Lee, S. C., D. E. Sabath, C. Deutsch, and M. B. Prystowsky. 1986. Increased voltage-gated potassium conductance during interleukin 2-stimulated proliferation of a mouse helper T lymphocyte clone. *Journal of Cell Biology.* 102:1200–1208.

Marty, A., and E. Neher. 1983. Tight-seal whole-cell recording. *In* Single Channel Recording. B. Sakmann and E. Neher, editors. Plenum Press, New York. 107–122.

Marty, A., and E. Neher. 1985. Potassium channels in bovine chromaffin cells. *Journal of Physiology.* 367:117–142.

Matteson, D. R., and C. Deutsch. 1984. K channels in T lymphocytes: a patch clamp study using monoclonal antibody adhesion. *Nature.* 307:468–471.

Murphy, E. E. 1981. Lymphoproliferation (*lpr*) and other single-locus models for murine lupus. *In* Immunologic Defects in Laboratory Animals. M. E. Gershwin and B. Merchant, editors. Plenum Press, New York. 2:143–173.

Nakajima, S. 1966. Analysis of K activation and TEA action in the supramedullary cells of puffer. *Journal of General Physiology.* 49:629–640.

Schlichter, L., N. Sidell, and S. Hagiwara. 1986. Potassium channels mediate killing by human natural killer cells. *Proceedings of the National Academy of Sciences.* 83:451–455.

Standen, N. B., P. R. Stanfield, and T. A. Ward. 1985. Properties of single potassium channels in vesicles formed from the sarcolemma of frog skeletal muscle. *Journal of Physiology.* 364:339–358.

Stanfield, P. R. 1983. Tetraethylammonium ions and the potassium permeability of excitable cells. *Reviews of Physiology, Biochemistry and Pharmacology.* 977:1–67.

Wofsy, D., E. D. Murphy, J. B. Roths, M. J. Duaphinee, S. B. Kipper, and N. Talal. 1981. Deficient interleukin 2 activity by MRL/Mp and C57BL/6J mice bearing the *lpr* gene. *Journal of Experimental Medicine.* 154:1671–1680.

Ypey, D. L., and D. E. Clapham. 1984. Development of a delayed outward-rectifying K^+ conductance in cultured mouse peritoneal macrophages. *Proceedings of the National Academy of Sciences.* 81:3083–3087.